Chemical Engineering Journal 104 (2004) 83–91

Chemical Engineering Journal

www.elsevier.com/locate/cej

Flow injection potentiometric stripping analysis for study of adsorption of heavy metal ions onto modified diatomite

Mohammad A. Al-Ghouti[a], Majeda A.M. Khraisheh[b,*], Maha Tutuji[c]

[a] *Industrial Chemistry Centre, The Royal Scientific Society, Amman, Jordan*
[b] *Department of Civil and Environmental Engineering, University College London, Gower Street, London WC1E 6BT, UK*
[c] *School of Chemistry, University of Jordan, Amman, Jordan*

Received 19 February 2004; received in revised form 12 July 2004; accepted 21 July 2004

Abstract

Computerised flow injection coupled with potentiometric stripping analysis (FIPSA) was employed for examination of the adsorption behaviour of Pb(II), Cd(II) and Zn(II) ions onto diatomite modified with manganese oxides. Signal optimisation was undertaken with respect to flow rate, deposition time, deposition potential, oxidising agent concentration, thickness of mercury film, solution pH and metal ion concentration. Examination of the column adsorption characteristics was facilitated by introduction of an adsorption microcolumn, as a complementary component of the flow injection system. The resulting breakthrough curves were employed to calculate parameters including adsorption capacity and adsorption rate constant, taking into consideration initial ion concentration, flow rate, mass and particle size of adsorbent, and column internal diameter. Adsorption capacities, determined using the Thomas mathematical model, showed that manganese modified Jordanian diatomite had an efficiency towards the removal of heavy metal ions from aqueous solutions; Cd(II) > Zn(II) ≈ Pb(II). The relative adsorption rates of the ions followed the order: Pb(II) > Zn(II) ≈ Cd(II).
© 2004 Elsevier B.V. All rights reserved.

Keywords: Adsorption; Diatomite; Flow injection; Heavy metals; Potentiometric; Stripping analysis

1. Introduction

Inorganic pollutants, in particular heavy metal ions, constitute a major class of water contaminants. Most heavy metals are known to be toxic and carcinogenic agents and, when discharged in wastewater, represent a serious threat to the human population. Currently, many industries use heavy metals in the processing of raw materials and consequently, discharge of such metals into aquatic bodies and sources of drinking water has begun to be strictly controlled [1]. Lead, cadmium and zinc are regarded as major contaminants. Lead and its compounds play an important role in industrial activities including the manufacture of paint, storage batteries and leaded gasoline. Cadmium and zinc are used as protective coatings for iron and steel. Cadmium enters the system primarily through absorption in the large intestine, and is deposited in the liver and kidneys [2]. Most zinc compounds have no toxic properties, but zinc chloride is highly corrosive to the skin, eye and respiratory tract.

Over the last few decades, adsorption has gained importance as an effective purification and separation technique used in wastewater treatment [3]. Adsorption systems are rapidly gaining prominence as treatment processes which produce good quality water containing a low concentration of dissolved organic and inorganic compounds [4]. Sorption technologies, including physical and chemical adsorption, and ion-exchange, have the potential to treat water and industrial residues.

The removal of heavy metals from industrial wastewater is considered an important application of adsorption processes using a suitable adsorbent [5]. There is growing interest in using low-cost, commercially available material for adsorption of heavy metals. Jordan has large deposits of diatomaceous earth and as a result, research is being undertaken to assess its feasibility as a low-cost alternative to activated carbon.

* Corresponding author. Tel.: +44 20 7679 7994; fax: +44 20 7380 0986.
E-mail address: m.khraisheh@ucl.ac.uk (M.A.M. Khraisheh).

1385-8947/$ – see front matter © 2004 Elsevier B.V. All rights reserved.
doi:10.1016/j.cej.2004.07.010

Diatomite is a siliceous, sedimentary rock consisting principally of the fossilised skeletal remains of the diatom, where the silica of the fossilised diatom skeleton resembles opal or hydrous, silica in composition ($SiO_2 \cdot nH_2O$). The diatomite has unique physical and chemical properties, which make it suitable for a wide range of applications. Its low bulk density, high surface area and low thermal conductivity are attributes responsible for its use as a functional filler, thermal insulator and catalyst carrier, as well as a substrate for adsorption of organic pollutants and some heavy metals. Al-Degs et al. [6] studied the capability of Jordanian diatomaceous earth (diatomite) as a potential adsorbent for Pb(II) ions. The intrinsic exchange properties were further improved by modification with manganese oxides. Modified adsorbent by manganese oxides showed a higher tendency for adsorbing lead ions from solution. The high performance exhibited by modified diatomite was attributed to increased surface area and higher negative surface charge after modification. Therefore, in this study, manganese oxides modified diatomite has been used as an adsorbent for heavy metal removal by using column studies.

The need for trace metal analysis, in particular, for the determination of lead, cadmium and zinc, is well documented [7]. A wide variety of techniques are employed in trace metal analysis; atomic absorption spectroscopy and inductively coupled plasma are accepted as standard methods. Efforts to enhance sensitivity and detection limits of electroanalytical methods have resulted in stripping analysis techniques being the most sensitive for the determination of heavy metal ions in trace concentrations [8]. Potentiometric stripping analysis is similar to conventional (voltammetric) stripping analysis in that the metals are pre-concentrated as amalgams in thin mercury film. However, it differs from voltammetric stripping modes in the approach used to reoxidise the metals and generate the analytical signals. Stripping techniques, particularly in the voltammetric mode, have been extensively applied to the analysis of heavy metal ions in environmental matrices; this is especially due to their excellent sensitivity which allows assessing the low metal concentrations frequently encountered [9,10]. La Pera et al. [11] demonstrated that hydrochloric acid extraction followed by derivative potentiometric stripping analysis (PSA) was a rapid, sensitive and precise method to determine simultaneously trace concentrations of Cd(II), Cu(II), Pb(II), and Zn(II) in oily matrices and the glassy carbon mercury-coated working electrode was well suited for this purpose.

Flow analytical techniques have also attracted attention in recent years [12]. In particular, the application of the flow injection (FI) to the electrochemical determination of metals in water sample, and adsorption behaviour on adsorbents using a microcolumn, by means of an automated, computerised system, has been reported to be an attractive proposition [12–14]. In particular, enhanced sample throughput and selectivity of trace metal determination can be achieved by combining such systems. This combination is characterised by injection of the sample into the delivery system and controlling dispersion of the sample, using the concept of 'limited' dispersion in FI to permit pre-concentrating of the sample. This can be achieved by plating in one electrolyte and stripping in another electrolyte for selectivity enhancement. The theory of the process was presented by Alex et al. [12] and Valcarcel and Castro [15].

The objective of this work is to develop a procedure to examine the adsorption of Pb(II), Cd(II) and Zn(II) onto manganese oxides modified diatomite (Mn-diatomite) using a microcolumn and flow injection (FI) coupled with potentiometric stripping analysis (PSA), taking into consideration the variables of initial ion concentration, adsorbate flow rate, mass and particle size of adsorbent, and column dimensions. Work on non-modified diatomite (in its raw state) is not considered in this particular paper which focuses only on modified diatomite. Some information on raw diatomite can be seen in Al Ghouti et al. [16].

2. Experimental

2.1. Adsorbent and adsorbates

The diatomite samples used in this study were obtained from the Al-Azraq area in East Jordan. Before use, the diatomite was washed with deionised water and, after being dried in an oven overnight at 100 °C, allowed to cool in a desiccator. Manganese oxide modification of the diatomite was accomplished by treatment with manganese chloride and sodium hydroxide. The procedures adopted are outlined in the work of Moore and Reid [17]. Stock solutions (100 mg l^{-1}) of Pb(II), Cd(II) and Zn(II) were prepared by dilution with deionised water. Metal nitrate was used in this study.

2.2. Flow injection potentiometric striping analyser (FIPSA) system

Potentiometric stripping analysis (PSA) is a two-step technique consisting of an electrolysis step and a stripping step. The electrolysis step, commonly performed using a mercury-film-coated glassy carbon electrode, is a pre-concentration step in which metal ions are reduced to free metal and electrodeposited as amalgam on the working electrode. The measurements are made in the stripping step during which the metal is reoxidised. The reoxidation can be a chemical or electrochemical process. During the stripping phase in the chemical oxidation, the electric circuit is interrupted and a chemical oxidant, such as dissolved oxygen or mercury ions, establishes the reoxidation. In electrochemical oxidation, an anodic current is imposed on the electrode to reoxidate the electrodeposited metals. The change in the electrode potential (E) over time (t) during the reoxidation process is monitored. A stripping potentiogram, E versus t, is obtained [18,19]

The FIPSA system consists of the operational section comprising the FI and the detection section, i.e. PSA. A micro-

column has been introduced into the system. A peristaltic pump is used to pump the solution, at a predetermined rate, through the column and into the flow cell. The flow cell is a three electrode system: (i) working electrode with a thin mercury film deposited on a highly polished glassy carbon electrode (GCE) disk embedded in polyvinylidene fluoride, (ii) reference electrode (Ag–AgCl) in a 3 M NaCl solution separated from the working electrode by a space (also acts as outlet channel), and (iii) counter stainless steel electrode (Fig. 1). Further details of the electrode preparation procedures adopted are given in Al-Ghouti [18].

The processing unit consists of a computer (for control and programming) and potentiostat/galvanostat to regulate the electrolysis voltage between the working glassy carbon electrode and counter electrode. The actual voltage between the GCE and reference electrode is displayed on a digital meter. Glass microcolumns of 10 cm length and selected internal diameters were used. Each column was filled with modified diatomite, and then the adsorbent packed into the microcolumn and positioned vertically between the peristaltic pump and flow cell (see Fig. 2).

2.3. Flow injection potentiometric stripping analysis – signal optimisation

Prior to each analysis, the used mercury film was wiped off with a tissue and the electrode cleaned with deionised water. Instrument signal optimisation for Pb(II), Cd(II) and Zn(II) ions was carried out with respect to the stripping potential range (identification interval, ID), deposition potential, deposition time, oxidising agent (Hg(II)) concentration, flow rate, pre-plating time (thickness of mercury film), pH of metal solution and metal ion concentration.

Table 1
Experimental variables used in signal optimisation

Variables	Experimental conditions
Metal concentration ($mg\,l^{-1}$)	1–4
Flow rate ($ml\,min^{-1}$)	1, 1.9, 2.7, 3.5
Temperature ($^{\circ}C \pm 1$)	23
Deposition time (s)	20, 50, 80, 100
Rest period (s)	40
pH	1–11
Concentration of oxidising agent (Hg(II)) ($mg\,l^{-1}$)	25, 50, 75, 100
Plating time (mercury-film thickness) (s)	120, 180, 240, 300

An arbitrary potential range from 220 to 10 mV was selected and the stripping signal for each analyte examined. The effect of deposition potential on the stripping signal was investigated from −0.2 to −1.2 V (at regular intervals of 0.1 V) and at −1.4 V, under the experimental conditions detailed in Table 1. Using the experimental conditions detailed in Table 1, the effect of deposition time, flow rate, pre-plating time, solution pH, and oxidising agent concentration on the stripping signal was investigated for selected Pb(II) concen-

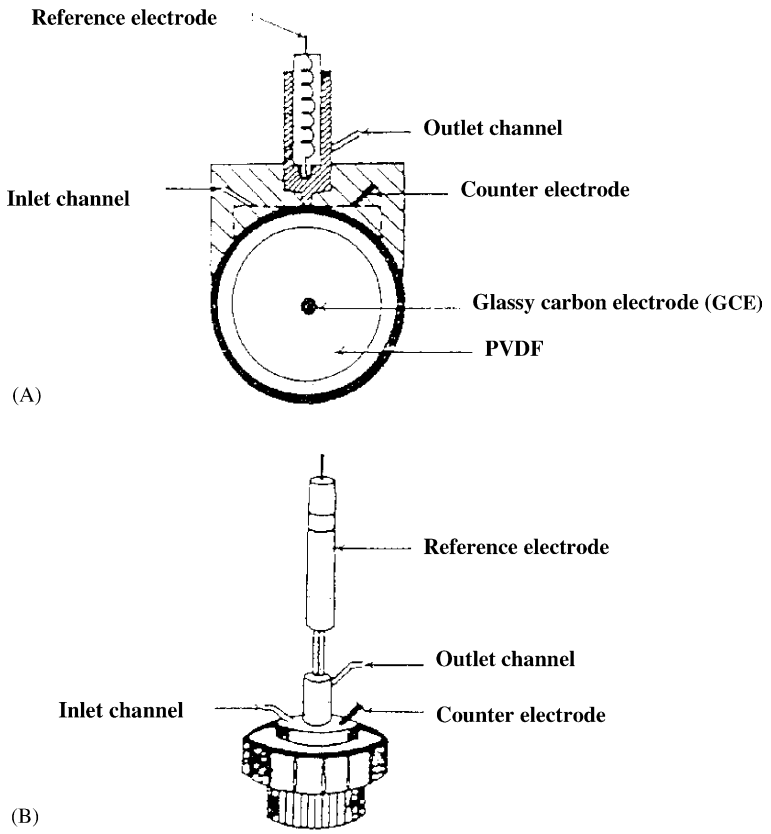

Fig. 1. Schematic representation of potentiometric stripping analyser flow cell: (A) opened cell showing the glassy carbon electrode; (B) closed cell.

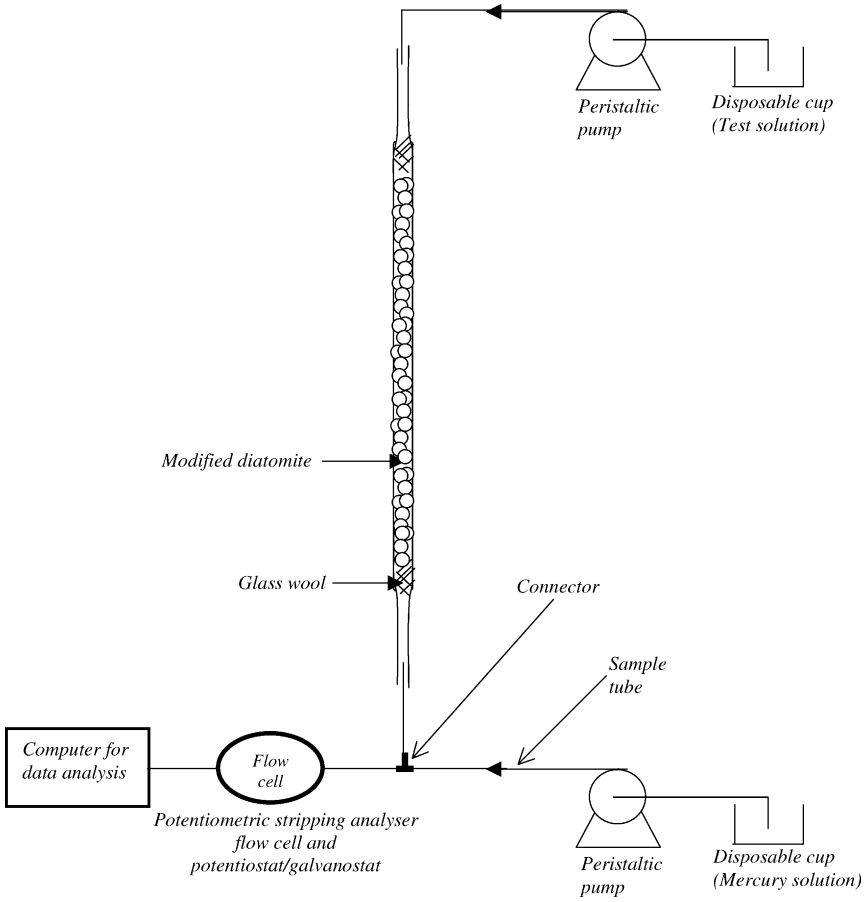

Fig. 2. Schematic representation of microcolumn adsorption of the heavy metals onto Mn-diatomite.

trations at an optimum potential of −0.9 V versus Ag/AgCl. The applied deposition potential to form a homogeneous stable mercury film is approximately −0.95 V versus Ag/AgCl [20].

The calibration curves for Pb(II), Cd(II) and Zn(II) were constructed by measuring the analyte signals for metal ion solutions of concentration 0–1, 1–10 and 10–30 mg l^{-1}, respectively, at the optimum deposition potentials. The precision and accuracy of the procedure for metal ion detection was also examined. Four samples of standard solutions were used. The standard deviation for measurements on low concentration lead, cadmium and zinc solutions were found to be less than 0.05. At high concentrations, the standard deviations of lead, cadmium and zinc were less than 2, 0.8 and 0.3, respectively. The detection limits were also established, based on the assumption that the smallest stripping signal was 80. Detection limits of 0.10, 0.22 and 0.06 mg l^{-1} were found for lead, cadmium and zinc, respectively. Further details are given in Al-Ghouti [18].

2.4. Flow injection potentiometric stripping analysis – microcolumn adsorption studies

A detailed study of the column adsorption characteristics of Pb(II), from the aqueous solution onto Mn-diatomite was facilitated by introduction of an adsorption microcolumn, as a complementary component of the flow injection system. Fig. 2 illustrates a schematic representation of microcolumn adsorption onto Mn-diatomite. The microcolumns were randomly filled with Mn-diatomite samples. Air pockets formed in the column could lead to channeling, increase in pressure drop and premature breakthrough due to the air pockets reducing the surface available for mass transfer between the Mn-diatomite and the metal solution. To solve this problem, deionised water was used to wash the Mn-diatomite sample in order to remove air bubbles and to rinse the Mn-diatomite. Moreover, metal solution with different concentrations was continuously fed to the top of the column at various flow rate controlled by a peristaltic pump (Watson–Marlow, 101U).

The experiments were carried out with respect to the parameters of initial ion concentration, flow rate, mass and particle size of adsorbent and column internal diameter, as summarised in Table 2. The FIPSA system was operated under the conditions identified during the signal optimisation experiments. A further evaluation of the column adsorption breakthrough curves for the heavy metal cations, Cd(II) and Zn(II), was also undertaken under the optimised operational conditions established during the Pb(II) experiments, as summarised in Table 3.

Table 2
Experimental variables for adsorption experiments for lead removal on Mn-diatomite using FIPSA technique

Variation adsorbent	Initial concentration ($mg\,l^{-1}$)	Mass of adsorbent (g)	Flow rate ($ml\,min^{-1}$)	Column internal diameter (cm)	Particle size (μm)
Initial concentration ($mg\,l^{-1}$)	5–20	0.1	2.7	0.2	<100
Adsorbent mass (g)	10	0.1–0.25	2.7	0.2	<100
Flow rate ($ml\,min^{-1}$)	10	0.154	1.0–3.5	0.2	<100
Column internal diameter (cm)	10	0.154	1.9	0.2–0.4	<100
Particle size (μm)	10	0.154	1.9	0.2	<100–315

3. Results and discussion

3.1. Flow injection potentiometric stripping analysis – signal optimisation

The identification potential interval is an arbitrary scale which signifies the stripping potential window. Each metal has a characteristic range indicative of the initiation and termination of chemical oxidation of the amalgamated metal. The optimum identification intervals for Pb(II), Cd(II) and Zn(II) were found to be 55–45, 80–70 and 125–115 mV, respectively.

The deposition potential is applied to the working thin mercury-film electrode, to selectively deposit the metal analyte onto the electrode surface. Pb(II) stripping remained constant in the range −0.7 to −0.9 V versus Ag/AgCl and Cd(II) in the potential range −0.8 to −0.9 V versus Ag/AgCl. Zn(II) signals, however, remained constant between −1.35 and −1.40 V versus Ag/AgCl. Thus, on the basis of the desired selectivity, optimum potentials of −0.9 V versus Ag/AgCl for Pb(II) and Cd(II), and −1.4 V versus Ag/AgCl for Zn(II) were chosen.

The deposition step is usually carried out by controlled potential electrolysis for a defined time, under reproducible hydrodynamic (mass transport) conditions. As reported in the literature [9], the stripping signals generated were directly proportional to the deposition time and the metal ion concentration. Thus, the longer the deposition time, the greater the amount of analyte moieties available to the electrode surface during the deposition and reduction steps. However, long deposition times are undesirable as this may cause the formation of intermetalic compounds, or saturate the thin mercury film [20]. In addition, bulk depletion of the analyte may occur with long deposition periods in dilute solutions. Thus, an optimum deposition time of 50 s was chosen.

Table 3
Summary of optimum operation conditions for the microcolumn

Parameter	Condition
Analyte concentration ($mg\,l^{-1}$)	10.0
Flow rate ($ml\,min^{-1}$)	1.9
Adsorbent mass (g)	0.1540
Column internal diameter (cm)	0.2
Particle size (μm)	<100

Conditions chosen on the basis of breakthrough curve shape, FIPSA signal stability and adsorption capacity. The shape of the breakthrough curve shape and stability of the FIPSA signal stability were considered more important than adsorption capacity, as these two criteria govern the precision of the analytical procedure.

In accordance with previous work [18] the Pb(II) stripping signal was found to be inversely proportional to Hg(II) concentration, i.e. at low mercury concentration the sensitivity of the PSA measurement was high. Faster oxidation rates were associated with lower analytical signals and lower sensitivities. Therefore, an optimum oxidising agent concentration was selected.

As expected [12], the Pb(II) stripping signal was shown to be inversely proportional to flow rate, irrespective of metal type and concentration. At reduced flow rates, both stripping and measurement sensitivity was high. At higher flow rates, oxidation of the amalgamated metal is controlled by the transport of Hg(II) ions towards the working electrode and as a result, lower sensitivities are expected for faster oxidation rates. However, faster flow rates cannot provide sufficient time to plate more metal [20]. At low flow rates, the rate of chemical oxidation is expected to be controlled by the rate of diffusion of the oxidant, Hg(II), to the surface and as a result, enhanced sensitivity is anticipated. Thus, an optimum flow rate of 1.9 $ml\,min^{-1}$ was adopted.

The mercury-film electrode consists of a thin layer of mercury on an inert support. The electrode offers a large surface-area-to-volume ratio, which provides a high amalgam concentration during the deposition step. As a result of the high plating efficiency, high selectivity is obtained, with the mercury film giving superior selectivity due to rapid diffusion from the bulk of the film to the surface [20]. The stripping signal was found to increase with pre-plating time (mercury-film thickness) up to 180 s and then remain constant. Thus, to obtain a consistent thin mercury film, plating was carried out in three cycles, each of duration 60 s.

Variation in pH can affect the quantity of metal ions accessible to the electrode, during both reduction and oxidation processes. From pH 1 to 5, solution pH had a negligible influence on the measurement, however, above pH 5 the stripping signals decreased. This may be explained by the possibility of precipitation as hydroxide(s). Furthermore, peak shapes improved at lower pH values. Consequently, a pH value of approximately 1, in a hydrochloric acid solution, was adopted in this work for Pb, Cd and Zn. This low value of pH was also used to study the adsorption parameters of Pb, Cd and Zn onto Mn-diatomite. However, a high pH value will be used in the next publications for determining the adsorption parameters of the system, since the pH of zero point of charge (p_{HZPC}) of

Table 4
Calibration curves of Pb(II), Cd(II) and Zn(II) at different concentrations ranges [$\ln((C_0/C_t)-1) = k_T q_0 m/F - (k_T C_0/F)V$]

Concentration range ($mg\,l^{-1}$)	Pb(II)			Cd(II)			Zn(II)		
	Slope ($k_T C_0/F$)	Intercept ($k_T q_0 m/F$)	R^2	Slope ($k_T C_0/F$)	Intercept ($k_T q_0 m/F$)	R^2	Slope ($k_T C_0/F$)	Intercept ($k_T q_0 m/F$)	R^2
0–1.0	0.813	0	0.972	1.692	0	0.959	0.801	0	0.981
1.0–10.0	0.373	0.687	0.981	0.940	1.386	0.974	0.826	−0.008	0.999
10.0–30.0	0.073	3.316	0.994	0.340	6.948	0.983	0.819	−2.923	1.000

Mn-diatomite is 2.2 [21]. This means that at higher pH value than 2.2, the surface of Mn-diatomite will be negative; hence higher adsorption. This procedure could be achieved by introducing a four-way valve which allows switching between different solutions. As a result, the metal solutions existing from the column, having different pH values, will change to pH = 1 by introducing a specific concentration of HCl.

Irrespective of metal type, Pb(II), Cd(II) and Zn(II), a linear relationship was observed between the stripping signal and ion concentration. Table 4 details the parameters for the first order equation fitted to the experimental data. As indicated, the lower the concentration range, the higher the calibration sensitivity. During the deposition step, when the concentration of the metal is low, the metal is uniformly distributed at the surface of the mercury film and thus, it is easy to oxidise the amalgamated metal during the stripping and dissolution steps. However, when the concentration of the metal is high, it may dissolve and distribute to the bulk of the mercury film, particularly if it is relatively thick. As a result, it may be difficult to oxidise the metal and subsequently, the sensitivity of measurement is reduced.

3.2. Flow injection potentiometric stripping analysis – microcolumn adsorption studies

Using Pb(II) as the model analyte, the factors affecting adsorption onto a microcolumn packed with diatomite modified with manganese oxides within the flow injection system were investigated (Table 5), and the optimum conditions to ensure the best operation of the experimental set-up, in terms of accuracy, precision and detection limits, established.

Adsorption involves interface accumulation, or concentration, of an adsorbate species at an adsorbent surface, or interface [22]. In a fixed bed adsorption system, the adsorbent located closest to the pollutant wastewater inlet is the first to become saturated (i.e. to reach equilibrium). Just downstream of the standard zone is a region of partial concentration gradient, which is referred to as the mass transfer zone. As time progresses, the adsorption zone moves further into the system, and then approaches the exit of the bed. When the adsorption zone has moved through the column, the concentration of the outlet adsorbate will be equal to that at the inlet. This process is described by a breakthrough curve.

Several factors affect the shape of a breakthrough curve, including physical and chemical properties of the adsorbent and adsorbate, solute concentration, adsorbent particle size, packed bed density, column depth, adsorbate flow rate, pH, temperature and nature of the equilibrium conditions [23].

Thomas derived the mathematical expression for a column with a typical breakthrough curve [24]

$$\frac{C_t}{C_0} = \frac{1}{1+\exp[k_T(q_0 m - C_0 V)/F]} \quad (1)$$

$$\Rightarrow \ln\left(\frac{C_0}{C_t} - 1\right) = \frac{k_T q_0 m}{F} - \frac{k_T C_0}{F} V \quad (2)$$

where C_0 is the initial dye concentration (mg/dm^3), C_t is the equilibrium concentration (mg/dm^3) at time t (min), k_T is the Thomas constant ($dm^3/min\,mg$), F is the volumetric flow rate (dm^3/min), q_0 is the maximum column adsorption capacity (mg/g), m is the mass of adsorbent (g) and V is the throughput volume (dm^3).

Hence a plot of $\ln((C_0/C_t) - 1)$ versus V gives a straight line with a slope of $(-k_T C_0/F)$ and an intercept of $(k_T q_0 m/F)$. Therefore, k_T and q_0 can be obtained.

The Thomas equation is one of the most general and widely used methods to predict the adsorption process [25].

Table 5
Adsorption capacity (Q) and rate constant (K_L) of lead adsorption on Mn-diatomite using Thomas model

Parameter	Adsorption capacity, Q ($mg\,g^{-1}$)	k_T ($dm^3\,min^{-1}\,mg^{-1}$)	R^2
Initial lead concentration ($mg\,l^{-1}$)			
5	1.08	0.0680	0.988
10	1.65	0.0524	0.983
15	4.59	0.0246	0.945
20	4.94	0.0264	0.939
Flow rate ($ml\,min^{-1}$)			
1.0	0.67	0.0721	0.898
1.9	1.57	0.0429	0.983
2.7	1.65	0.0524	0.976
3.5	1.67	0.0577	0.971
Mass of adsorbent (g)			
0.1013	1.52	0.0429	0.983
0.1470	1.02	0.0656	0.970
0.1920	9.88	0.0403	0.986
0.2400	8.28	0.0392	0.987
Internal column diameter (cm)			
0.2	1.02	0.0656	0.983
0.3	0.85	0.0319	0.967
0.4	0.47	0.0380	0.939
Particle size (μm)			
<100	1.02	0.0656	0.983
125	0.95	0.0299	0.918
315	0.93	0.0391	0.946

The Thomas model, which assumes Langmuir kinetics of adsorption–desorption and no axial dispersion, is derived with the assumption that the rate driving force obeys second-order reversible reaction kinetics. Thomas solution also assumes a constant separation factor but it is applicable to either favourable or unfavourable isotherms. The primary weakness of the Thomas solution is that its derivation is based on second-order reaction kinetics. Adsorption is usually not limited by chemical reaction kinetics but is often controlled by interphase mass transfer. This discrepancy can lead to some error when this method is used to model adsorption process [25].

The effect of initial dye concentration on the shape of the breakthrough curves and the column adsorption parameters was investigated. Fig. 3 depicts the breakthrough curves of adsorption of Pb(II) onto Mn-diatomite at different initial dye concentrations as a plot of dimensionless concentration (C_t/C_0) versus volume (V) of metal treated. As shown from the breakthrough curves in Fig. 3, adsorption capacity increases with initial lead concentration. This can be explained by the fact that more adsorption sites are being covered as the adsorbate concentration increases. This is also due to the concentration gradient. Higher initial dye concentrations lead to a higher concentration gradient, hence the mass transfer driving force will be higher [26]. Further analysis of the data in terms of adsorption capacity, Q (Eq. (2), Table 5), reveals that the sites are fully covered when the adsorption level reaches 15 mg l^{-1}. The kinetic parameter, rate constant (K_L), predicted by the model, was found to be affected by initial Pb(II) concentration, with its value decreasing from 0.068 to 0.0264 $dm^3\ min^{-1}\ mg^{-1}$ as the initial lead concentration changed from 5 to 20 mg l^{-1}. The increase of Pb(II) concentration results in an increase in the driving force, which will enhance the diffusion rate of the metal ion in pores.

In column studies contact time is the most significant variable and therefore bed depth and metal flow rate are the major parameters [27]. Consequently, adsorption of Pb(II) was studied at different flow rates in order to investigate the effect of flow rate on the adsorption behaviour. Initial metal concentration, pH and particle size were maintained constant. As shown in Fig. 4 andTable 5, the lead adsorption

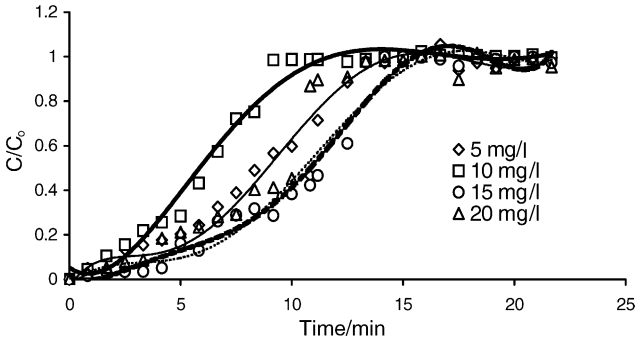

Fig. 3. Breakthrough curves of lead adsorption onto Mn-diatomite using different lead concentrations.

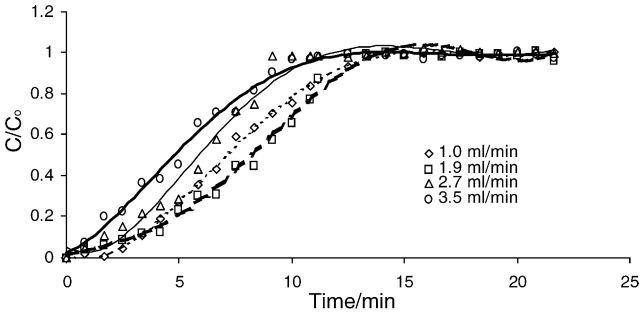

Fig. 4. Breakthrough curves of lead adsorption onto Mn-diatomite using different flow rates.

characteristics are dependent on adsorbate flow rate. The adsorption capacity increases with increasing flow rate up to 2.7 ml min^{-1}, having a value of 1.65 g g^{-1}, and then remains approximately constant for higher flow rates. Therefore, a flow rate of 2.7 ml min^{-1}, or above, ensures full coverage of all adsorption sites. The Thomas mathematical model predicts that the rate constant, K_L, increases with adsorbate flow rate; 0.0429 to 0.0577 $dm^3\ min^{-1}\ mg^{-1}$. A large value of the rate constant indicates that the adsorption capacity will reach the equilibrium value faster. This could be explained as (i) a higher flow rate decreases the external film mass resistance at the surface of the adsorbent and (ii) the resistance time of the metal ions inside the bed deceases with higher flow rate hence the time that is required to diffuse and penetrate into the centre of the adsorbent is lower [25,26].

The observed breakthrough curves of Pb(II) for Mn-diatomite at four different masses of adsorbent are displayed in Fig. 5, plotted as the effluent concentration ratio versus the throughput volume. As detailed in Table 5, there is no obvious relationship between adsorption capacity and adsorbent mass. Such behaviour may be explained in terms of differences in adsorbent particle packing. In the low mass region, loose packing is obtained, while in the high mass region there is compact packing and therefore, the adsorbate solution has more contact within the adsorbent surface. The data shown in Table 5 indicates that the adsorption constant, K_L, does not vary significantly with adsorbent mass.

Fig. 6 and Table 5 depict the effect of column internal diameter on lead adsorption breakthrough curves. The ad-

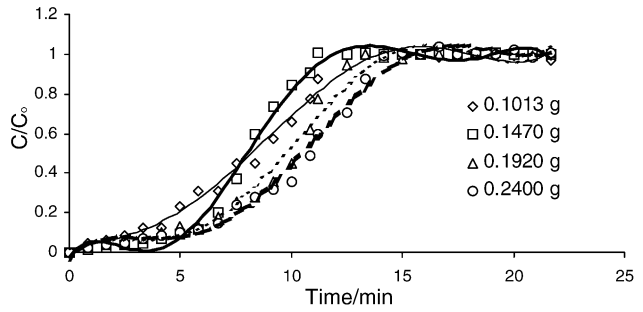

Fig. 5. Breakthrough curves of lead adsorption onto Mn-diatomite using different masses of Mn-diatomite.

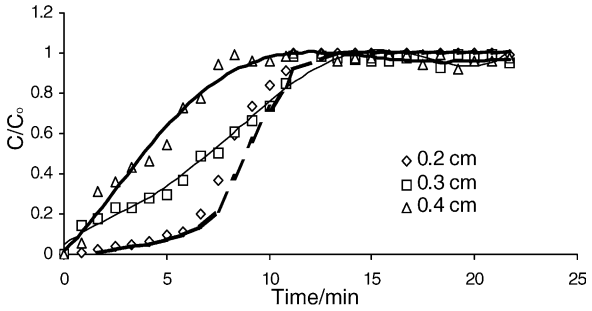

Fig. 6. Breakthrough curves of lead adsorption onto Mn-diatomite using different internal column diameters.

sorption capacity decreases with increasing column internal diameter due to the fact that the adsorption sites have not been covered completely in columns of increased internal diameter. Furthermore, it is easier for equilibrium to be attained when the adsorbent is well packed in a smaller diameter column. This behaviour is in accordance with observations regarding the influence of adsorbent mass. The rate constant K_L, exhibited no relation with column internal diameter; such behaviour may also be explained in the terms of the adsorbent particle packing.

Examination of the effect of adsorbent particle size on the adsorption characteristics indicates that the adsorption capacity decreases slightly with increasing adsorbent particle size (Fig. 7 and Table 5). This may be due to the fact that the adsorption is a surface phenomenon and as such, the extent of adsorption is expected to be proportional to the specific surface. However, the loose packing of the adsorbent may have compensated for the effect of particle size on adsorption in the flow system. Thus, the rate and extent of lead adsorption decreased by increasing the particle size. It can be attributed to the relationship between the effective specific surface area and size of the adsorbent particles. Effective surface area decreases as particle size increases and as a consequence, the saturation adsorption per unit mass of adsorbent decreases [5,28].

Adopting the optimised operational conditions established for Pb(II), which were also found to work well for Cd(II) and Zn(II), a study of the adsorption rates and adsorption capacity of aqueous solutions of the heavy metal ions onto

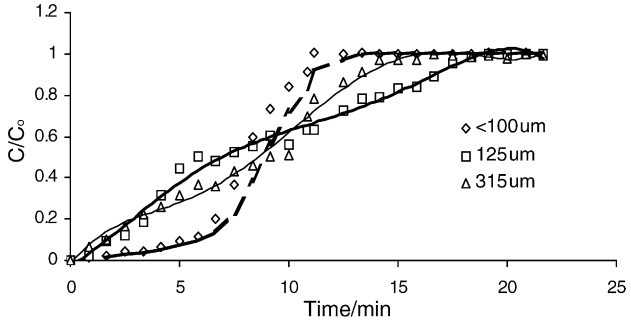

Fig. 7. Breakthrough curves of lead adsorption onto Mn-diatomite using different particle sizes.

Table 6
Adsorption capacity (Q) and rate constant (K_L) of lead, cadmium and zinc adsorption on Mn-diatomite using Thomas model

Analyte	Adsorption capacity, Q (mg g^{-1})	k_T (dm^3 min^{-1} mg^{-1})	R^2
Pb(II)	1.02	0.0656	0.983
Cd(II)	1.23	0.0350	0.985
Zn(II)	1.05	0.0354	0.971

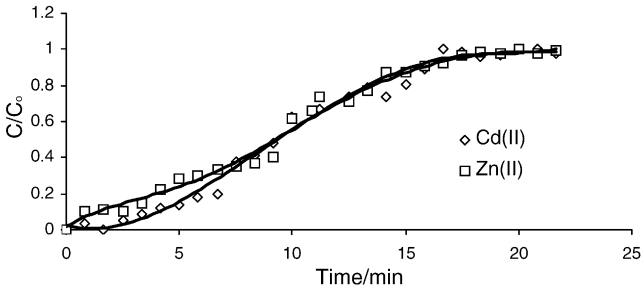

Fig. 8. Breakthrough curves of adsorption of Cd(II) and Zn(II) onto Mn-diatomite.

Mn-diatomite was undertaken. The adsorption characteristics are summarised in Table 6 and Fig. 8. Examination of the adsorption capacities for Pb(II), Cd(II) and Zn(II), derived from the Thomas mathematical model (Table 6), indicates that manganese modified Jordanian diatomite has an efficiency towards the removal of these heavy metal ions from aqueous solutions. The adsorption capacity of cadmium onto Mn-diatomite is found to be higher than that for lead and zinc, with the relative adsorption capacities following the sequence: Cd(II) > Zn(II) ≈ Pb(II). The adsorption capacity variation reflects the equilibrium state of the adsorbate on the surface, which is governed by the ionic radius and isomorphic substitution. Cd(II) is isomorphic with Ca(II) and Na(I), which together are the most abundant exchangeable ions present in the mineral matrix. The adsorption rate, K_L, of cadmium was lower than that of lead and zinc. Thus, the adsorption rate follows the sequence: Pb(II) > Zn(II) ≈ Cd(II). The behaviour of the adsorption rate, being the kinetic parameter, is affected by the force field of the cations which in this case is the highest for Pb(II).

4. Conclusions and further work

Different acid and base concentrations have been used to study the desorption efficiency on heavy metal/Mn-diatomite. Different eluants, lowering or rising solution temperature might help to regenerate the adsorbent. Mechanisms of metal adsorption onto Mn-diatomite will be studied in the next publications in addition to the effect of the existence of manganese and mercury ions in the adsorption process. The manganese ions may dissolve from Mn-diatomite adsorbent at low pH, thus, the adsorption process could be affected.

However, on the basis of the experimental and theoretical results of this investigation, the following conclusions

can be drawn:

- The proposed flow injection potentiometric stripping analysis system, employed for adsorption using a microcolumn, proved efficient.
- The Thomas mathematical model adequately described the adsorption of Pb(II), Cd(II) and Zn(II) onto Mn-diatomite.
- Manganese modified Jordanian diatomite had an efficiency towards the removal of Pb(II), Cd(II) and Zn(II) ions from aqueous solutions.
- The relative adsorption capacities of the heavy metal ions onto Mn-diatomite followed the sequence: Cd(II) > Zn(II) ≈ Pb(II).
- The relative adsorption rates of the ions followed the order, Pb(II) > Zn(II) ≈ Cd(II).

References

[1] T.N. De Castro Dantas, A.A. Neto, M.C. Moura, Removal of cadmium from aqueous solutions by diatomite with microemulsion, Water Res. 35 (9) (2001) 2219–2224.

[2] M.G. Holliday, J.M. Park, Canadian kidney-cadmium levels, exposure and environmental control, in: Proceedings of the Air and Waste Management Association's Annual Meeting and Exhibition, 1998, p. 14.

[3] N.K. Lazaridis, T.D. Karapantsios, D. Georgantas, Kinetic analysis for the removal of a reactive dye from aqueous solution onto hydrotalcite by adsorption, Water Res. 37 (2003) 3023–3033.

[4] G.M. Walker, L.R. Weatherley, Kinetic of acid dye adsorption on GAC, Water Res. 33 (8) (1999) 1895–1899.

[5] Z. Al-Qodah, Adsorption of dyes using shale oil ash, Water Res. 34 (17) (2000) 4295–4303.

[6] Y. Al-Degs, M.A.M. Khrasisheh, M.F. Tutunji, Sorption of lead ions on diatomite and manganese oxides modified diatomite, Water Res. 35 (15) (2001) 3724–3728.

[7] T.R. Copeland, R.K. Skogerboe, Anodic stripping voltammetry, instrumentation, Anal. Chem. 46 (14) (1974) 1257A–1266A.

[8] E. Sahlin, D. Jagner, R. Ratana-ohpas, Mercury nucleation on glassy carbon electrodes, Anal. Chim. Acta 346 (2) (1997) 157–164.

[9] D. Jagner, M. Josefson, S. Westerlund, Determination of zinc, cadmium, lead and copper in sea water by means of computerized potentiometric stripping analysis, Anal. Chim. Acta 129 (1) (1981) 153–161.

[10] D. Jagner, Potentiometric stripping analysis for mercury, Anal. Chim. Acta 105 (1) (1979) 33–41.

[11] L. La Pera, F. Lo Coco, E. Mavrogeni, D. Giuffrida, G. Dugo, Determination of copper(II), lead(II), cadmium(II) and zinc(II) in virgin olive oils produced in sicily and apulia by derivative potentiometric stripping analysis, Ital. J. Food Sci. 14 (2002) 389–399.

[12] H. Alex, E.D. Raymond, G. Auders, Potentiometric stripping with matrix exchange techniques in flow injection analysis of heavy metals in ground waters, Anal. Chem. 55 (1983) 320–328.

[13] C.K. Polydorou, C.E. Efstathiou, Microcomputer controlled system for potentiometric stripping analysis, Anal. Instrum. 20 (4) (1992) 265–283.

[14] Z.L. Chen, P.W. Alexander, Potentiometric flow-injection analysis of alkali and alkaline metals with a tungsten oxide coated film sensor, Lab. Robotics Automat. 9 (4) (1997) 201–206.

[15] M. Valcarcel, M.D.L. Castro, Flow Injection Analysis. Principles and Applications, 1st ed., Wiley, New York, 1987.

[16] M.A. Al-Ghouti, M.A.M. Khraisheh, S.J. Allen, M.N. Ahmad, The removal of dyes from textile wastewater: a study of the physical charachterstics and adsorption 15 mechanisms of diatomaceous earth, J. Environ. Manage. 69 (2003) 229–238.

[17] W.S. Moore, D.F. Reid, Extraction of radium from natural water using manganese-impregnated acrylic fibres, J. Geophys. Res. 78 (1973) 8880–8886.

[18] M.A. Al-Ghouti, Development of a flow injection method for studying adsorption processes, and to investigate its use in the removal of some water pollutants, Master Degree in Chemistry (Thesis), University of Jordan, Amman, Jordan, 1999.

[19] E. Muñoz, S. Palmero, M.A. García-García, A continuous flow system design for simultaneous determination of heavy metals in river water samples, Talanta 57 (2002) 985–992.

[20] W. Joseph, Stripping Analysis: Principles, Instrumentation and Application, 1st ed., VCH, Florida, 1985.

[21] M.A.M. Khraisheh, M.A. Al-Ghouti, S.J. Allen, M.N.M. Ahmad, The effect of pH, temperature and molecular size on the removal of dyes from textile effluent using manganese oxides-modified diatomite. Water Environ Res. 76 (6) (2004) 51–59.

[22] C.W. Cheung, J.F. Porter, G. McKay, Sorption kinetic analysis for removal of cadmium ions from effluents using bone char, Water Res. 35 (3) (2001) 3147–3152.

[23] L.M. Alan, B. Georges, Fundamentals of Adsorption, American Institute of Chemical Engineers, 461-469, 929-936 and 679-692, 1984.

[24] L. Conter, R. Knox, Ground Water Pollution Control, Lewis, New York, 1986, pp. 96–101.

[25] Z. Aksu, F. Gönen, Biosorption of phenol by immobilised activated sludge in a continuous packed bed: prediction of breakthrough curves, Process Biochem. 39 (2004) 599–613.

[26] V.K.C. Lee, J.F. Porter, G. McKay, Development of fixed-bed absorber correlation models, Ind. Eng. Chem. Res. 39 (2000) 2427–2433.

[27] K.H. Chu, Improved fixed bed models for metal biosorption, Chem. Eng. J. 97 (2004) 233–239.

[28] K. Banergee, P.N. Cheremisinoff, L.S. Cheng, Adsorption kinetics of *o*-xylene by flyash, Water Res. 31 (1997) 249–261.